polymer. In ferritin, the polymerization process could be regulated by access channels through the protein sheath and by phosphate anions. The latter are possible pH regulators. They may also serve to link crystallites that result during the polymerization process and act as counterions. The ratio of phosphate:iron may also be important in regulating the size of the crystallites. A higher number of phosphates results in smaller crystallites and a lower degree of crystallinity of the core.[6i,47–50]

In the formation of **1**, the phenyl rings may play the role of the protein sheath, but only up to its hydrophobic surface, with carboxylate groups anchored to it. A binuclear $\{Fe_2O\}^{4+}$ complex could bind to the carboxylate groups, forming Hr-like structures. Unlike Hr, the hollow apoferritin core allows subsequent addition of metal atoms to the initial complex, a possible first step in this direction being modeled by the $\{Fe_3O\}^{7+}$ and $\{Fe_4O_2\}^{8+}$ type complexes.[16–18] Slow addition of H_2O favors oligomerization as well as introduction of hydroxyl groups.

The structure of the $[Fe_{11}O_6(OH)_6(O_2CPh)_{15}]$ molecule reveals only octahedral coordination around iron, in agreement with the optical and near IR spectroscopy of ferritin; the magnetic and Mössbauer properties are also similar, but not identical. Preliminary electrochemical studies by cyclic voltammetry indicate that *the aggregate* can be reversibly reduced by one electron, compared with the one electron *per iron* reduction of mammalian ferritin.[46] The presence of THF or MeCN hydrogen bonded to the Fe_{11} core suggests a manner by which small molecules could facilitate the removal of iron from the ferritin core in accord with recent suggestions.[51,52] The phenyl rings form six rudimentary "channels" that may provide size and hydrophilic/hydrophobic selection for the "attacker", the same way that the ferritin protein sheath does.

Acknowledgment. This work was supported by National Institute of Health Research Grant GM 31234 (to S.J.L.) from the National Institute of General Medical Sciences. R.B.F. and G.C.P. were supported by the Office of Naval Research. The Francis Bitter National Magnet Laboratory is supported by the National Science Foundation. We thank R. L. Rardin and M. Hostettler for experimental assistance.

Supplementary Material Available: Tables of thermal parameters for all atoms, hydrogen positional and thermal parameters, and a full list of bond lengths and angles (18 pages); listing of observed and calculated structure factor amplitudes (74 pages). Ordering information is given on any current masthead page.

---

(47) Macara, I. G.; Hay, T. G.; Harrison, P. M. *Biochem. J.* **1972**, *126*, 151–162.

(48) Stiefel, E. I.; Watt, G. D. *Nature (London)* **1979**, *279*, 81–83.

(49) Mansour. A. N.; Thomson, C.; Theil, E. C.; Chasteen, N. D.; Sayers, D. E. *J. Biol. Chem.* **1985**, *260*, 7975–7979.

(50) Watt, G. D.; Frankel, R. B.; Papaefthymiou, G. C.; Spartalian, K.; Stiefel, E. I. *Biochemistry* **1986**, *25*, 4330–4336.

(51) Funk, F.; Lenders, J.-P.; Crichton, R. R.; Schneider, W. *Eur. J. Biochem.* **1985**, *152*, 167–172 and references cited therein.

(52) Jones, T.; Spencer, R.; Walsh, C. *Biochemistry* **1978**, *17*, 4011–4017.

Identification and Structural Implications of the 90 K Superconducting Phase†

H. Steinfink,* J. S. Swinnea, Z. T. Sui,‡ H. M. Hsu, and J. B. Goodenough

Contribution from the Center for Materials Science and Engineering, The University of Texas at Austin, Austin, Texas 78712. *Received March 30, 1987*

Abstract: The phase relations of Cu-containing compounds in the system Y_2O_3–BaO–CuO were determined at a temperature of about 950 °C and a fixed partial pressure of 0.21 atm of oxygen. Mixtures of Y_2O_3, $BaCO_3$, and CuO were heated and the products identified by powder X-ray diffraction. The stable ternary phases containing Cu are $Y_2Cu_2O_5$, Y_2BaCuO_5, $YBa_2Cu_3O_{8-y}$, and $BaCuO_2$. The 90 K superconducting material is $YBa_2Cu_3O_{8-y}$. It is an ordered phase and does not display detectable solid solution between Y and Ba. It is orthorhombic $a = 3.824$ (1) Å, $b = 3.891$ (1) Å, $c = 11.685$ (2) Å. A pseudotetragonal structure based on $a \approx b \approx 3.87$ Å, $c = 11.68$ Å, $P4/mmm$ has Y situated between square coplanar CuO_2 layers; there are no oxygen atoms at this level. In the stoichiometry $YBa_2Cu_3O_8$ the copper between Ba layers occupies a tetragonally distorted octahedron ($c/a = 0.88$). It is most likely that the oxygen vacancies are associated with this Cu–O octahedral layer in $YBa_2Cu_3O_{8-y}$. The dramatic increase in superconducting transition temperature on going from the K_2NiF_4 structure of $La_{2-x}Ba_xCuO_{4-y}$ to the $YBa_2Cu_3O_{8-y}$ structure is considered with reference to large bipolarons, the position of the d_{z^2} energy level relative to the Fermi energy, and the overlap of the Cu:3d and O:2p bands.

Following the initial report of Bednorz and Müller[1] of evidence for high-temperature ($T_c > 30$ K) superconductivity in a La–Ba–Cu–O mixed-phase system, numerous workers[2–4] identified the superconducting phase as $La_{2-x}M_xCuO_{4-y}$ (M = Ba, Sr, or Ca) having the tetragonal K_2NiF_4 structure. Although the initial work was stimulated by an earlier paper[5] on the oxygen-defect perovskites $La_{3-x}Ln_xBa_3[Cu^{II}_{5-2y}Cu^{III}_{1+2y}]O_{14+y}$, primary theoretical attention has been focused on phases based on the K_2NiF_4 structure.

For a variety of reasons, several groups have substituted yttrium for lanthanum in an attempt to make $Y_{2-x}M_xCuO_{4-y}$ analogues; these efforts resulted in a multiphase product in which an unidentified phase gave a superconducting transition temperature

---

[†] The Experimental and Results sections were presented at the American Crystallographic Association Meeting, March 16, 1987 in Austin, Texas.

[‡] Northeast University of Technology Shenyang, People's Republic of China, Visiting Scientist.

(1) Bednorz, J. G.; Müller, K. A. *Z. Phys.* **1986**, *B64*, 189.

(2) (a) Takagi, H.; Uchida, S.; Katazawa, K., Tanaka, S. *Jpn. J. Appl. Phys. Lett.* **1987**, *26*, L123. (b) Uchida, S.; Takagi, H.; Tanaka, S.; Katazawa, K. *Jpn. J. Appl. Phys. Lett.*, in press. (c) Cava, R. J.; van Dover, R. B.; Battlog, B.; Rietman, E. A. *Phys. Rev. Lett.* **1987**, *58*, 408.

(3) Tarascon, J. M.; Greene, L. H.; McKinnon, W. R.; Hall, G. W.; Geballe, T. H. *Science* **1987**, *235*, 1373.

(4) Jorgensen, J. D.; Schuttler, H.-B.; Hinks, D. G.; Capone, D. W.; Zhang, K.; Brodsky, M. B.; Scalapino, D. J. *Phys. Rev. Lett.* **1987**, *58*, 1024.

(5) Er-Rakho, L.; Michel, C.; Provost, J.; Raveau, B. *J. Solid State Chem.* **1981**, *37*, 151.

0002-7863/87/1509-3348$01.50/0

Table I. Phase Relations 920–1000 °C

	composition mole fraction			reaction conditions			
no.	$YO_{1.5}$	BaO	CuO	temp, °C	time, h	products	remarks
1	0.21	0.13	0.67	1000	48	$Y_2BaCuO_5 \simeq CuO > YBa_2Cu_3O_x$	samples 1–3 reground after 24 h reaction time
2	0.16	0.16	0.67	1000	48	$YBa_2Cu_3O_x = CuO > Y_2BaCuO_5$	
3	0.13	0.20	0.67	1000	48	$YBa_2Cu_3O_x > CuO \gg Y_2BaCuO_5$	
4	0.10	0.40	0.50	950	20	$YBa_2Cu_3O_x > BaCuO_2$	
5	0.115	0.385	0.50	920	18	$YBa_2Cu_3O_x > BaCuO_2$	
6	0.125	0.375	0.50	950	32	$YBa_2Cu_3O_x > BaCuO_2$	
7	0.13	0.37	0.50	920	18	$YBa_2Cu_3O_x > BaCuO_2$	
8	0.15	0.35	0.50	950	20	$YBa_2Cu_3O_x \gg BaCuO_2$	
9	0.165	0.335	0.50	950	20	$YBa_2Cu_3O_x$	
10	0.18	0.32	0.50	920	18	$YBa_2Cu_3O_x > CuO = Y_2BaCuO_5$	
11	0.20	0.30	0.50	950	20	$YBa_2Cu_3O_x > Y_2BaCuO_5 > CuO$	
12	0.25	0.25	0.50	920	18	$YBa_2Cu_3O_x > Y_2BaCuO_5 > CuO$	
13	0.30	0.20	0.50	950	20	$Y_2BaCuO_5 > YBa_2Cu_3O_x > CuO$	
14	0.45	0.05	0.50	950	20	$Y_2Cu_2O_5 = Y_2BaCuO_5 \gg CuO$	
15	0.40	0.27	0.33	950	36	$Y_2BaCuO_5 > YBa_2Cu_3O_x > CuO$	reground after 12 h
16	0.33	0.33	0.33	950	36	$Y_2BaCuO_5 > YBa_2Cu_3O_x$	possibility of $BaCO_3$
17	0.40	0.20	0.40	1000	36	$Y_2BaCuO_5 > CuO$	reground after 12 h

$T_c > 90$ K.[6-8] In this paper we report that the phase responsible for this extraordinary superconductivity has a structure related to the tetragonal defect-perovskite structure first worked out from powder data for $La_3Ba_3Cu_6O_{14.1}$.[5] We also discuss a theoretical basis for experimental strategies in this field.

Experimental Section

Y_2O_3, CuO, and $BaCO_3$ were used as the starting materials with nominal purities of 99.99, 99.9, and 99.8, respectively. The starting materials were single-phase as judged by their X-ray powder diffraction patterns. Mixtures varying between 50 and 1000 mg were prepared by grinding the components in hexane or acetone, drying them, and then firing them for 24 h in platinum or zirconia crucibles at 925–1000 °C in air. The samples were air-quenched by removing them from the furnace. Some of the fired specimens were reground after 12 h of heating and then refired. All products were examined with an optical microscope, and the X-ray powder diffraction patterns were obtained with a diffractometer fitted with a diffracted-beam graphite monochromator and Cu Kα radiation. Magnetic susceptibility measurements were carried out with a Faraday balance from room temperature to pumped liquid N_2.

Results

The phase relations among the stable phases in the Y_2O_3–BaO–CuO system over the temperature interval 925–1000 °C shown in Figure 1 were established from the results of 17 equilibrium experiments. The experimental results are listed in Table I. Samples 1–3 and 15–17 were reacted in a tube furnace where temperature gradients of 100 °C were present over the length of the ZrO_2 boat. The highest temperature is shown in the table. Samples 4–14 were reacted in a muffle furnace, and temperatures are ±20 °C.

At most three phases can coexist in this system when the temperature and the partial pressure of O_2 (0.21 atm) are fixed. The JCPDS X-ray diffraction data file[9] contained information that permitted the identification of $Y_2Cu_2O_5$, $BaCuO_2$, as well as the starting materials, but it was evident that in many of the products there were unidentified diffraction lines that were due to two unknown phases, the superconducting compound and an additional Y–Ba–Cu oxide.

We carried out a search for all Y–Cu compounds contained in the NBS inorganic data base using CRYSTDAT.[10] In addition to $Y_2Cu_2O_5$ we found Y_2BaCuO_5, a structure reported by Michel and Raveau as orthorhombic.[11] The lattice constants yielded "*d*" spacings that accounted for many of the unidentified lines. We also prepared this compound, and its powder pattern is reported in Table II. We now had the information needed to identify two of the three possible phases; these two were not superconducting, so that the remaining unidentified lines had to be from the superconducting phase.

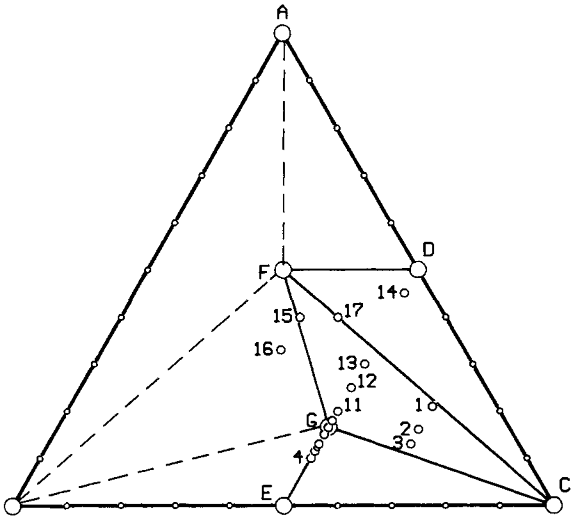

Figure 1. Phase relations at 925–1000 °C. Intervals on the diagram are in 10% and are denoted by very small circles. A = $YO_{1.5}$, B = BaO, C = CuO, D = $Y_2Cu_2O_5$, E = $BaCuO_2$, F = Y_2BaCuO_5, G = $YBa_2Cu_3O_{8-y}$.

The product resulting from the mixture number 9 was single-phase and corresponded to the superconducting compound as judged by the X-ray powder diffraction pattern. A tabular crystal about 50 μm in size was selected and mounted on a Weissenberg camera. Oscillation and zero- and first-level Weissenberg diagrams were obtained. The crystal was twinned. The oscillation photograph showed intensities on layer lines slightly separated parallel to the oscillation axis. Ignoring these separations, an average value of the periodicity of 3.8 Å was obtained. With this the *a* axis, a 0*kl* Weissenberg photograph showed two spots from each reflection 0*kl* except 00*l*. The *c* axis obtained from this photograph was 11.68 Å. The 1*kl* photograph showed split spots except for the reciprocal lattice row 11*l*. Another crystal was now mounted along the *c* axis; the layer lines contained pairs of spots and all *hk*0 reflections of the Weissenberg photograph were doubled except when *h* = *k*. The lattice constants measured from these photographs were *a* = 3.810 Å, *b* = 3.874 Å, *c* = 11.68 Å. The twinning results from the 90° rotation of the reciprocal lattice

---

(6) Chu, C. W.; Hor, P. H.; Meng, R. L.; Gao, L.; Huang, Z. J.; Wang, Y. Q.; Bechtold, J.; Campbell, D.; Wu, M. K.; Ashburn, J.; Huang, C. Y. *Phys. Rev. Lett.*, submitted for publication.

(7) Wu, M. K.; Ashburn, J. R.; Torng, C. J.; Hor, P. H.; Meng, R. L.; Gao, L.; Huang, Z. J.; Wang, Y. Q.; Chu, C. W. *Phys. Rev. Lett.* **1987**, *58*, 908.

(8) Tarascon, J. M.; Greene, L. H.; McKinnon, W. R.; Hull, G. H. *Phys. Rev. Lett.*, submitted for publication.

(9) JCPDS: International Centre for Diffraction Data, 1601 Park Lane, Swarthmore PA 19081.

(10) CRYSTDAT: Canada Institute for Scientific and Technical Information, National Research Council of Canada, Ottawa, Canada K1A 0S2.

(11) Michel, C.; Raveau, B. *J. Solid State Chem.* **1982**, *43*, 73.

Table II. Powder X-ray Diffraction Pattern for Y_2BaCuO_5[a]

hkl	$2\theta_{obsd}$ (deg)	$2\theta_{calcd}$ (deg)	d_{obsd} (Å)	I_{obsd}
200	14.568	14.543	6.075	2.0
111	21.331	21.329	4.162	2.0
020	24.987	24.970	3.561	2.2
120	26.055	26.036	3.417	6.0
220	29.038	29.016	3.073	4.7
400	29.379	29.327	3.038	5.8
311	29.872	29.839	2.989	100.0
121	30.556	30.525	2.923	60.4
002	31.655	31.619	2.824	44.1
410	31.797	31.955	2.796	16.3
221	33.148	33.136	2.700	17.8
320	33.460	33.443	2.676	1.7
202	34.934	34.964	2.566	5.3
411	35.776	35.771	2.508	12.2
321	37.132	37.125	2.419	8.5
230	40.753	40.743	2.212	20.5
031	41.181	41.186	2.190	5.4
122	41.416	41.404	2.178	10.1
131	41.881	41.878	2.155	6.7
511	42.352	42.331	2.132	3.4
402	43.678	43.665	2.071	7.6
600	44.642	44.632	2.028	8.1
412	45.583	45.571	1.989	34.0
322	46.687	46.687	1.944	6.3
521	47.899	47.998	1.894	2.7
430	48.585	48.584	1.872	10.1
611	49.363	49.371	1.845	3.5
113	50.629	50.609	1.802	1.9
512	51.094	51.103	1.786	9.1
431	51.347	51.361	1.778	5.8
140	51.822	51.822	1.763	6.9
232	52.459	52.468	1.743	16.3
710	54.240	54.258	1.690	2.4
621	54.459	54.476	1.684	5.3
313	55.184	55.213	1.663	14.8
123	55.630	55.632	1.651	11.5
711	56.825	56.837	1.619	3.9
223	57.265	57.284	1.608	4.0
720	59.096	59.068	1.562	12.2

Table III. Powder X-ray Diffraction Pattern for $YBa_2Cu_3O_{8-y}$[a]

hkl	d_{calcd} (Å)	d_{obsd} (Å)	I_{rel}
001	11.685	11.868	1
002	5.843	5.875	2
003	3.895	3.897	11
010	3.891		
100	3.824	3.828	3
012	3.238	3.235	4
102	3.200	3.200	4
004	2.921	2.926	1
013	2.753	2.750	62
103	2.729	2.727	100
110	2.727		
111	2.656	2.649	1
112	2.471	2.472	4
005	2.337	2.338	13
014	2.336		
104	2.321	2.318	2
113	2.234	2.236	17
015	2.003	1.997	1
105	1.994		
114	1.994		
006	1.948	1.946	22
020	1.945		
200	1.912	1.911	14
115	1.775	1.775	4
016	1.742	1.738	3
023	1.740		
106	1.735		
120	1.734		
203	1.716	1.715	2
210	1.716		
121	1.715		
007	1.669	1.668	1
122	1.662	1.661	1
212	1.646	1.647	1
116	1.585	1.584	33
123	1.584		
213	1.570	1.570	14
025	1.495	1.494	3
124	1.491		
205	1.480	1.480	3
214	1.480		
117	1.424	1.424	2
026	1.376	1.376	4
018	1.368	1.364	12
108	1.365		
206	1.364		
220	1.364		
009	1.298	1.295	1
030	1.297		
126	1.295		
031	1.289	1.287	2
118	1.288		
216	1.288		
223	1.287		

[a] The lattice constants $a = 3.824$ (1) Å, $b = 3.891$ (1) Å, $c = 11.685$ (2) Å were obtained from a least-squares refinement of the indexed "*d*" values.

Table IV. Positional Parameters for the Idealized Tetragonal Structure of $YBa_2Cu_3O_{8-y}$ based on *P*4/*mmm* and $a = 3.87$ Å, $c = 11.68$ Å

atom	Wyckoff notation	*x*	*y*	*z*
Cu 1	1a	0	0	0
Cu 2	2g	0	0	0.347
Y	1d	1/2	1/2	1/2
Ba	2h	1/2	1/2	0.180
O 1	2f	0	1/2	0
O 2	4i	0	1/2	0.358
O 3[a]	2g	0	0	0.147

[a] Partial occupancy.

around *c*. Such twinning is often encountered when two lattice constants have similar values.

We assumed a pseudotetragonal unit cell and initiated a search of the inorganic data base[10] for all rare-earth or scandium or yttrium oxides that have diffraction symmetry 4/*mmm*. This search produced eight matches. One of them, $La_3Ba_3Cu_6O_{14.1}$,[5] confirmed the result of the phase diagram study for the stoichiometry of the superconducting phase, $YBa_2Cu_3O_{8-y}$; it also indicated that the structure was ordered. When we prepared mixtures that deviated even slightly from the (Y + 2Ba)/Cu = 1:1 ratio, a second phase appeared; e.g., for the 0.3Y:0.7Ba:1Cu (number 8) a second phase, $BaCuO_2$, was seen in addition to the superconducting compound. It was evident that if a range of solid solubility existed at all between Y and Ba, it was extremely small. The powder X-ray diffraction pattern for $YBa_2Cu_3O_{8-y}$ is shown in Table III. The assignment of Miller indices to the diffraction lines in Tables II and III and the least-squares refined values of the lattice constants shown there were obtained with the program TREOR[12] and a locally written program.

Er-Rakho et al.[5] determined the crystal structure of $La_3Ba_3Cu_6O_{14.10}$ from powder diffraction data choosing a tetragonal unit cell with twice the volume of our pseudotetragonal cell. The Miller indices in their Table III are $h + k = 2n$ for all observed *hkl* so that their Bravais lattice should be C centered rather than P as given. This caused them to list atoms as crystallographically independent that are not. The doubled cell volume is a consequence of the inclusion of a single line, 100, so faint that d_{obsd} is not reported, only d_{calcd} with I_{obsd} = vw and I_{calcd} = 0.3 (most intense I_{calcd} = 71.3). The existence of this line is problematical, and its omission leaves all other *hkl* indices $h + k = 2n$. However, the structure shown in their Figure 3 is closely related to that of the superconducting $YBa_2Cu_3O_{8-y}$. We surmise that the oxygen vacancies introduce small distortions in the structure that lower

---

(12) Werner, P.-E.; Eriksson, L.; Westdahl, M. *J. Appl. Crystallogr.* **1985**, *18*, 367.

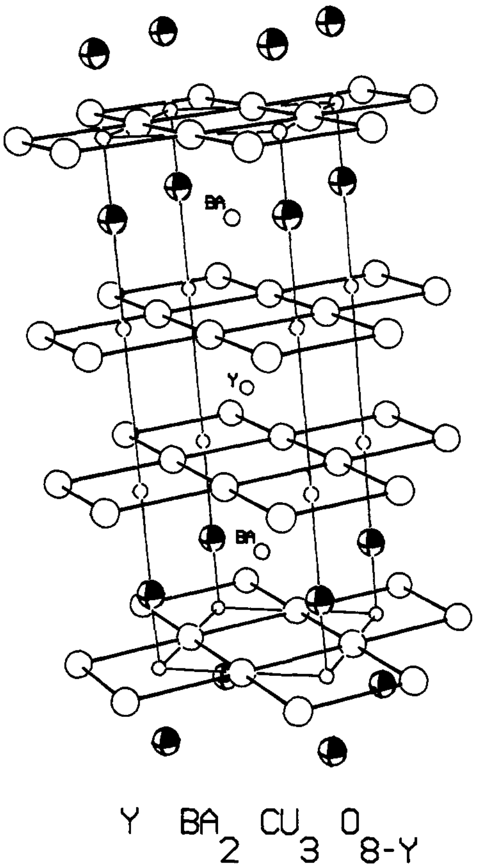

Figure 2. Idealized tentative structure of the "tetragonal" $YBa_2Cu_3O_{8-y}$ phase. Shaded circles represent O(3); open circles are O(1) and O(2); and the small circles are Cu(1) and Cu(2). The *c* axis is vertical.

the crystal system to orthorhombic. Since they were unable to determine the distribution of La and Ba in the structure, they prepared $La_2YBa_3Cu_6O_{14+y}$ and found that (1La + 1Y) preferentially ordered into one site while (3Ba + 1La) ordered in another site.

This result showed that Y and Ba did not share the same crystallographic position in the structure. We, therefore, placed Y and Ba into the positions shown in Table IV using an idealized tetragonal structure in $P4/mmm$. The coordinates are derived from those reported by Er-Rakho et al.[5] but recalculated for the primitive cell. A drawing of the structure is shown in Figure 2. The Y^{3+} ions are located between the essentially square-coplanar Cu(2)–O layers, and no oxygen ions are present in the Y level. Ba^{2+} is located between the square-coplanar (or square pyramidal) level and the octahedral Cu(1)–O level. The oxygen vacancies are associated with the Cu(1) atoms. We are unable to distinguish whether the vacancies are in the O(3) or O(1) or both sites. The Cu(1)–O(3) bond length is about 1.72 Å. The Cu(2)–O(3) bond length is about 2.33 Å. The c/a ratio of the Cu(1)–O octahedron is 0.88, which would be consistent with O(1) vacancies. It is interesting to note that this ratio is 1.82 for the distorted octahedron in the La_2CuO_4 structure[13] (Cu–apical O = 2.46 Å) while in Nd_2CuO_4 the apical O has moved into a new position, a tetrahedral site,[14] and there are indeed true Cu^{2+}–O planar nets, but all Cu is divalent in this structure.

Use of the phase-diagram information from Figure 1 made straightforward the interpretation of the X-ray powder pattern published by Tarascon et al.[8] for the product resulting from the nominal composition $Y_{2-x}Ba_xCuO_{4-y}$, $x = 0.25$. They identified two phases, Y_2O_3 and $Y_2Cu_2O_5$, whose powder X-ray diffraction patterns are present in the JCPDS data file.[9] At least two more phases were indicated by an asterisk and a circle over a number of lines in their diagram labeled Figure 2. Their Table 1a listed a series of lines that were observed in this mixture as well as in mixtures from $x = 0.20$ and 0.15. This is the Y_2BaCuO_5 phase. Their Table 1b lists four lines that were visible only in the $x = 0.25$ product. We identified the last two lines in this table as due to CuO, and the weak 2.745 and 2.721 Å lines are from the superconducting phase. It is interesting to note that the second most intense line of Y_2BaCuO_5, $d = 2.92$ Å, 60% intensity, superimposes on the $d = 2.94$ Å line of $Y_2Cu_2O_5$, 30% intensity, and makes it too intense to be only due to $Y_2Cu_2O_5$ as indicated in their diffraction diagram.

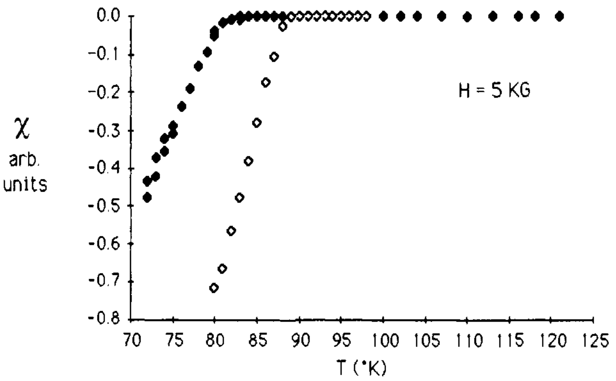

Figure 3. Magnetic susceptibilities in arbitrary units vs. *T* of single-phase superconducting powders: filled diamonds, air-quenched at 900 °C; open diamonds, annealed in O_2 at 400 °C for 8 h.

The superconducting behavior of the single-phase powder that we prepared by quenching from 950 °C was demonstrated by obtaining the magnetic susceptibility as a function of temperature, and Figure 3 shows the onset at about 80 K. The parameter of interest in Figure 3 is the onset of the transition below which superconductivity makes the material strongly dimagnetic. When the quenched material was annealed for 8 h at 400 °C in a flowing stream of O_2, the onset of the transition temperature was raised to nearly 90 K.

From these experiments we conclude that the superconducting phase is an ordered compound with the composition $YBa_2Cu_3O_{8-y}$. The superconductivity is due to the mixed valence state of copper, which is caused by the oxygen vacancies. The oxygen vacancies give rise to a small distortion of the structure, and this distortion changes the crystal system from tetragonal to orthorhombic. It should also be noted that, if this composition is referred to a perovskite structure, its idealized composition would be $YBa_2Cu_3O_9$, which would require oxygen atoms at the Y level. The absence of these oxygen changes the structure and composition sufficiently to consider this a new structure type.

Discussion

The striking structural feature common to both the $La_{2-x}M_xCuO_4$ (M = Ba, Sr, or Ca) and the $YBa_2Cu_3O_{8-y}$ phase of Figure 2 is the presence of CuO_2 planes containing exclusively 180° Cu–O–Cu coupling. This feature gives rise to three characteristics that have been noted and emphasized by one of us in earlier publications.[15-17]

1. Hybridization of Cu:d$_{x^2-y^2}$ and O:p$_\sigma$ Orbitals. The empty $Cu^{2+/+}$ redox level lies close enough to the top of the filled O^{2-}:$2p^6$ band that strong covalent mixing of the Cu:$d_{x^2-y^2}$ and in-CuO_2-plane O:p_σ orbitals occurs, where *z* is taken parallel to the *c* axis and *x*,*y* are oriented along the Cu–O–Cu bond axes in a CuO_2 plane. This hybridization extends the primarily Cu:$d_{x^2-y^2}$

---

(13) Grand, B.; Müller-Buschbaum, Hk.; Schweizer, M. *Z. Anorg. Allg. Chem.* **1977**, *428*, 120.

(14) Müller-Buschbaum, Hk.; Wollschlager, W. *Z. Anorg. Allg. Chem.* **1975**, *414*, 76.

(15) Goodenough, J. B. *Mater. Res. Bull.* **1973**, *8*, 423. Goodenough, J. B.; Demazeau, G.; Pouchard, M.; Hagenmuller, P. *J. Solid State Chem.* **1973**, *8*, 325.

(16) Goodenough, J. B. *Prog. Solid State Chem.* **1971**, *5*, 145. *Proceedings of the Climax 4th International Conference on Chemistry and Uses of Molybdenum*, Barry, M. F., Mitchell, P. C. H., Eds.; Climax Molybdenum Co.: Ann Arbor, MI, 1982; pp 1–23.

(17) Gleitzer, C.; Goodenough, J. B. *Struct. Bonding (Berlin)* **1985**, *61*, Chapter 1.

σ-antibonding wave functions out over the anions and raises their energy while lowering the corresponding primarily O:p$_\sigma$ σ-bonding states, which are (x^2-y^2)-symmetrized. The Cu–O antibonding states of $d_{x^2-y^2}$ parentage are denoted $\sigma^*_{x^2-y^2}$ to distinguish them from the Cu–O bonding states $\sigma_{x^2-y^2}$.

Extension of the "crystal-field" $d_{x^2-y^2}$ orbitals out over the anions by O:p$_\sigma$ hybridization has two important effects: it enhances the in-plane Cu–O–Cu interactions and lowers the interatomic electron–electron electrostatic interactions responsible for the correlation energy U. Consequently, the Cu-3d electron states of $d_{x^2-y^2}$ parentage become transformed into itinerant, one-electron states of a *narrow* $\sigma^*_{x^2-y^2}$ band even for the formal valence state Cu^{2+}. Further oxidation of the copper broadens this band.

2. Anisotropic Bonding. Any interplane Cu–O–O–Cu, Cu–O–Cu, or Cu–Cu interactions are much weaker. Therefore, although Cu–O hybridization reduces U for the d_{z^2} electrons also, any unpaired d_{z^2}-electron spins can be expected to introduce a spontaneous atomic moment and therefore quench the superconducting state. Therefore, the energy of the $d_{z^2}{}^2$ configuration relative to the middle of the narrow $\sigma^*_{x^2-y^2}$ band of itinerant-electron states becomes a critical consideration; it varies sensitively with the axial c/a ratio of a tetragonally distorted octahedral site occupied by copper. Only in a square-coplanar configuration would it appear safe to neglect the $d_{z^2}{}^2$ electrons for any Cu^{3+}/Cu^{2+} ratio in a formal mixed-valence state.

3. Charge-Density Waves. A partially filled, narrow band of one-electron states having a bandwidth $w_b > U$, where U is the Hubbard intraatomic electron–electron electrostatic energy, may have its occupied states stabilized at the expense of unoccupied states by a lattice deformation that changes the translational periodicity. If the diffusionless deformation occurs below the melting point of the solid, the resulting standing wave of charge-density fluctuation is called a charge-density wave.

Two types of charge-density waves have been distinguished: atomic or ionic clustering and disproportionation. The former occurs where direct metal–metal or anion–anion interactions create the partially filled, narrow band; the latter occurs where the narrow band is assciated with 180° metal–anion–metal interactions, which is the situation for the $\sigma^*_{x^2-y^2}$ band in the CuO_2 layers under consideration.

Recent band calculations[4,18,19] for La_2CuO_4 accept as given the itinerant character of the $\sigma^*_{x^2-y^2}$ band and essentially ignore the $d_{z^2}{}^2$ configuration, placing it well below the Fermi energy E_F. This leaves the $\sigma^*_{x^2-y^2}$ band half-filled, which is the optimal situation for a disproportionation (negative U) charge-density wave in which the area of the unit cell in a CuO_2 layer is doubled; the two types of copper are distinguished by short vs. long Cu–O bonds in the basal plane. Shortening of a Cu–O bond raises the energy of the $\sigma^*_{x^2-y^2}$ orbitals; lengthening the bond lowers the energy. As a result there is a net electron transfer from the copper with shorter Cu–O bonds to those with longer Cu–O bonds: $Cu^{2+} + Cu^{2+} \rightarrow Cu_I{}^{(2+\delta)+} + Cu_{II}{}^{(2-\delta)+}$, $0 < \delta \leq 1$. Direct verification of such a deformation by diffraction techniques may be complicated by disordered phasing of the charge-density waves of successive CuO_2 planes on progressing along the c axis of the cell.

However satisfactory this model for the semiconducting state of La_2CuO_4, evidence for a weak, intrinsic atomic moment, which now appears spurious, suggested that some $d_{z^2}{}^2$ energies were intersected by E_F in that orthorhombic phase.[20] However, in the superconducting $La_{2-x}M_xCuO_{4-y}$ (M = Ba, Sr or Ca) phases, there is no magnetic moment associated with the copper, and the $d_{z^2}{}^2$ energy lies discretely below the middle of the $\sigma^*_{x^2-y^2}$ band; introduction of a mixed formal valence Cu^{3+}/Cu^{2+} by substituting an alkaline earth for some lanthanum suppresses formation of a standing charge-density wave even though the CuO_2 layer remains intact. This observation has prompted formulation of a disproportionation bipolaron model for the superconducting state.[21]

A Cooper pair consists of two spin-paired electrons bound by a mobile lattice deformation; the "dressed" electron pair moves as a boson with a well-defined momentum vector $\mathbf{k}$. It may be envisaged as a large bipolaron with a deformation corresponding to either atomic clustering or a disproportionation. Only the latter is applicable to the CuO_2 layers; and in this case the energy gained by trapping a pair of electrons in a mobile lattice deformation must be greater than the increased electrostatic energy U between the paired electrons. Hence the importance of a narrow band having a small U and the absence of any spontaneous atomic moment associated with the atoms whose orbitals participate in the narrow bands. Formation of the superconducting state requires condensation of large-bipolaron units (Cooper pairs) from states near the Fermi energy without the introduction of the long-range order characteristic of a charge-density wave. Such a condensation opens up an energy gap at the Fermi surface without changing the translational symmetry of the lattice.

Given this general picture, one important question emerges on comparing the structures of the $La_{2-x}M_xCuO_{4-y}$ (M = Ba, Sr, or Ca) and $YBa_2Cu_3O_{8-y}$ phases: Why should the superconducting transition temperature be limited to $T_c \leq 40$ K in the former but reach $T_c > 90$ K in the latter?

A clue may reside in the observation that all the copper in the $La_{2-x}M_xCuO_{4-y}$ phases occupy octahedral sites distorted to tetragonal ($c/a > 1$) symmetry whereas two-thirds of the copper in the $YBa_2Cu_3O_{8-y}$ phase occupy essentially square-coplanar sites.

As shown in Figure 2, the large Ba^{2+} ion would have a Ba–O distance incompatible with a Goldschmitt tolerance factor $t \leq 1$ were the O_3 oxygens in the same plane as the Ba. Consequently, the O_3 atoms are shifted along the c axis away from the CuO_2 planes neighboring the Y planes. The smaller Y^{3+} ions, on the other hand, are commonly found in eightfold oxygen coordination, so there is a complete lack of oxygen in the Y planes. The net result is that the CuO_2 planes neighboring the Y plane have copper in a square-pyramidal coordination that approaches only fourfold, square-coplanar coordination. The $d_{z^2}{}^2$ energies at the copper in these planes would lie lower relative to the midpoint of the $\sigma^*_{x^2-y^2}$ band than those of octahedral-site copper.

If the $d_{z^2}{}^2$ energy is not too far below the middle of the $\sigma^*_{x^2-y^2}$ band in a $La_{2-x}M_xCuO_{4-y}$ phase, then lowering of E_F by increasing x and/or decreasing y would cause E_F to intersect the $d_{z^2}{}^2$ level at some critical concentration x_c for $y \approx 0$. The fact that T_c exhibits a maximum as a function of x could be due to an $x \rightarrow x_c$. In this case, a square-coplanar configuration, which increases x_c to $x \approx 1$, would allow optimization of x at some maximum in the density-of-states vs. energy for the $\sigma^*_{x^2-y^2}$ band. The sensitivity of T_c to oxygen concentration in both phases indicates the importance of the position of E_F within the $\sigma^*_{x^2-y^2}$ band, and the dramatic enhancement of T_c on going from $La_{1.85}Ba_{0.15}CuO_4$ to $YBa_2Cu_3O_{8-y}$ suggests that lowering of the $d_{z^2}{}^2$ energies has allowed E_F to range more deeply into the $\sigma^*_{x^2-y^2}$ band, especially for lower values of y where T_c appears to be highest.

On the other hand, local charge neutrality would seem to favor locating the holes associated with the formal valence Cu^{3+} in the Cu(1) layers between Ba^{2+} ion planes for the oxygen stoichiometry $Ba_2YCu_3O_7$, and this stoichiometry is compatible with placing the oxygen vacancies at the O(1) sites. Contraction of the a axis suggests that the vacancies are on the a axis to give linear chains of coplanar CuO_4 groups corner-sharing along the b axis and lying in the (100) plane. The Cu(1)–O(3) terminal bonding would be stronger than the 180° Cu(1)–O(1)–Cu(1) bonding. In this configuration, the z axis at a Cu(1) may be taken parallel to the a axis, and introduction of additional oxygen ($Ba_2YCu_3O_{7+x}$) would allow cross-talk between chains via delocalized $d_{z^2}{}^{2-\delta}$ – O-$d_{z^2}{}^{2-\delta}$ bridges. Thus the CuO_{4-y} layers between Ba atom planes are structurally quite distinct from the CuO_2 planes of the $La_{1-x}M_xCuO_4$ structure; moreover, they appear to be responsible for the high superconductivity T_c.

A second clue resides in the extreme sensitivity of T_c to the total oxidation state. In view of the difficulty of preparing copper oxides

---

(18) Mattheiss, L. F. *Phys. Rev. Lett.* **1987**, *58*, 1028.

(19) Yu, J.; Freeman, A. J.; Xu, J.-H. *Phys. Rev. Lett.* **1987**, *58*, 1035.

(20) Singh, K. K.; Ganguly, P.; Goodenough, J. B. *J. Solid State Chem.* **1984**, *52*, 254.

(21) Prelovek, P.; Rice, T. M.; Zhang, F. C., personal communication.

in the formal valence state Cu^{3+} or even $Cu^{4+/3+}$ without the application of high oxygen pressure and/or the presence of a strongly electropositive ion like Ba^{2+}, it may be suspected that there is an important overlap of the $Cu{:}\sigma^*_{x^2-y^2}$ and O:2p bands. In such a case there is an alternative deformation, not previously considered, that can implement transfer of a disproportionation bipolaron from one copper center to another as a bipolaronic entity; it consists of Cu–O–Cu trimers that stabilize more O:2p hybridization in d-band bonding states (Cu–Cu bonding since these states are always antibonding with respect to the Cu–O interactions) and more Cu:3d character in the empty O:2p states. Thus formation of Cooper pairs instead of a charge-density wave may require that the Fermi energy intersect overlapping Cu:3d and O:2p bands.

Finally, the distinction between a Cooper pair as a large bipolaron and the small bipolaron originally identified[22] in Ti_4O_7 is worth pointing out. Ti_4O_7 consists of TiO_2 slabs between regularly spaced shear planes. Electrostatic repulsions between Ti^{4+} ions on either side of a shear plane introduce short Ti–O bonds at these ions; consequently the mobile electrons of this formally Ti^{4+}/Ti^{3+} mixed-valent system occupy titanium 3d-band states within the slabs. At lowest temperatures, these electrons condense out in an ordered array of Ti^{3+}–Ti^{3+} homopolar bonds across shared octahedral-site edges to form a standing charge-density wave. As the temperature is raised, there is a narrow temperature interval in which the dimers become disordered and mobile; at higher temperatures the electrons are not trapped but occupy normal narrow-band states. In this case, the mobile bipolarons move diffusively, so they have no meaningful **k** vector. These bipolarons do not condense out into a superconducting state. On the other hand, superconducting $Li[Ti_2]O_4$,[23] which has the spinel structure, undoubtedly has Cooper pairs in the superconducting state that are large bipolarons trapped in mobile Ti atom dimers or tetramers. Similarly, large disproportionation bipolarons must be distinguished from descrete formal valence states such as stationary Pb^{2+} ions condensed out, for example, of reduced PbO_2.

The analogy between the superconducting copper oxides and the superconducting $BaBi_xPb_{1-x}O_3$ perovskites[24] is close; but in the copper oxides the $\sigma^*_{x^2-y^2}$ band is not perturbed by substituting for copper whereas in $BaBi_xPb_{1-x}O_3$ the 6s band is strongly perturbed by substituting Bi for Pb.

The transition from mobile small bipolarons to Cooper pairs in mixed-valence systems as a function of bandwidth and band occupancy has never been adequately explored; it has been commonly assumed that either charge-density waves, which can be incommensurate, or diffusive small-bipolaron motion would always compete successfully with high-temperature superconductivity. It now appears that this assumption may not apply where the Fermi energy intersects two bands, one of which derives from an anion array and the other from a cation array.

Acknowledgment. We gratefully acknowledge the research support of the R. A. Welch Foundation of Houston, Texas. The first four authors also acknowledge support by the National Science Foundation under Grant DMR 8520028.

---

(22) Chakraverty, B. K. *J. Phys. Lett.* **1979**, *40*, L-99.

(23) Johnston, D. C. *J. Low-Temp. Phys.* **1976**, *25*, 145.

(24) Sleight, A. W.; Gillson, J. L.; Bielstedt, F. E. *Solid State Commun.* **1975**, *17*, 27.

Steric Effects, as well as σ*-Orbital Energies, Are Important in Diastereoface Differentiation in Additions to Chiral Aldehydes[1]

Eric P. Lodge and Clayton H. Heathcock*

Contribution from the Department of Chemistry, University of California,
Berkeley, California 94720. *Received November 20, 1986*

Abstract: Two series of chiral aldehydes (**5a–e** and **6a–d**) have been prepared and their aldol reactions with the lithium enolate of pinacolone examined. The observed diastereomer ratios (Table I) have been evaluated in terms of the Anh–Eisenstein interpretation of Felkin's model for 1,2-asymmetric induction. It is shown that the simple steric effects are at least as important as σ*-orbital energies in determining which is the "large" group for the purpose of applying the Felkin model. In all but the simplest cases, it is necessary to evaluate a four-conformer equilibrium in order to confidently predict the sense and magnitude of 1,2-asymmetric induction in such reactions. For a purely qualitative approach to predicting the major isomer produced in the series studied, one may use the Felkin model for 1,2-asymmetric induction with the following order of ligand preferences for the anti position: MeO > *t*-Bu > Ph > *i*-Pr > Et > Me > H. The results of this study cannot be rationalized by either the Cieplak hypothesis or the Ruch–Ugi stereochemical analogy model.

Relative asymmetric induction[2] in additions to chiral aldehydes and ketones is a topic of great interest. In a pair of pioneering papers published in the early 1950s, Cram[3] and Prelog[4] set forth models for predicting the major diastereomer to be expected in nucleophilic additions to chiral carbonyl compounds.[5]

Of these seminal contributions, the most valuable from a practical point of view was Cram's rule for asymmetric induction in additions to carbonyl groups having an adjacent stereocenter, which proved to be exceedingly useful in correlating a large amount of experimental data.[6] The original formulation of Cram's rule was "...that diastereomer will predominate which would be formed by the approach of the entering group from the less hindered side of the double bond when the rotational conformation of the C–C bond is such that the double bond is flanked by the two least hindered bulky groups attached to the asymmetric center."[3] This statement implies a one-conformer model (**1a**) with major and minor diastereomers resulting from attack on the less and more hindered carbonyl faces. However, in a later paper on the subject, Cram and Kopecky presented a Newman projection of the con-

---

(1) Part 40 in the series "Acyclic Stereoselection". For part 39, see: Lodge, E. P.; Heathcock, C. H. *J. Am. Chem. Soc.* **1987**, *109*, 2819.

(2) Bartlett, P. A. *Tetrahedron* **1980**, *45*, 2.

(3) Cram, D. J.; Abd Elhafez, F. A. *J. Am. Chem. Soc.* **1952**, *74*, 3210.

(4) Prelog, V. *Helv. Chim. Acta* **1953**, *36*, 308.

(5) An important insight into the problem of asymmetric induction in such reactions came in an earlier paper by Curtin and co-workers: Curtin, D. Y.; Harris, E. E.; Meislich, E. K. *J. Am. Chem. Soc.* **1952**, *74*, 2901.

(6) See, inter alia: (a) Morrison, J. D.; Mosher, H. S. *Asymmetric Organic Reactions*; Prentice-Hall: Englewood Cliffs, NJ, 1971; pp 84–132. (b) Eliel, E. L. In *Asymmetric Synthesis*; Morrison, J. D., Ed.; Academic: New York, 1983; Vol. 2, pp 125–156.

0002-7863/87/1509-3353$01.50/0